

A novel gradient climbing control for seeking the best communication point for data collection from a seabed platform using a single unmanned surface vehicle^{*}

Jiu-cai JIN^{†‡§}¹, Jie ZHANG¹, Zhi-chao LV^{1,2}

¹*First Institute of Oceanography, Ministry of Natural Resources, Qingdao 266061, China*

²*College of Underwater Acoustic Engineering, Harbin Engineering University, Harbin 150001, China*

[†]E-mail: jinjiucai@fio.org.cn

Received Nov. 7, 2017; Revision accepted Sept. 4, 2018; Crosschecked June 11, 2019

Abstract: A novel controller for finding the best communication point is proposed for collecting data from a seabed platform by a single unmanned surface vehicle (USV) using underwater acoustic communication (UAC). As far as we know, extremum seeking based on climbing control is usually implemented by multiple vehicles or agents because of the large range of measurement and easy acquisition of gradient estimation. A single vehicle cannot rapidly estimate the field because of the limited extent for measurement; therefore, it is difficult for a single vehicle to seek the extremum point in a field. In this study, an oscillation motion (OM) is designed for a single USV to acquire UAC's link strength data between the seabed platform and the USV. The field for UAC's link strength is updated using new measurement from an OM of the USV based on a multi-variable weight linear iteration method. A controller for seeking the best UAC's point of the USV is designed using gradient climbing and artificial potential considering iterative estimation of an unknown field and an OM operation, and the stability is proved. The reliability and efficiency are shown in simulation results.

Key words: Unmanned surface vehicle; Data collection; Underwater acoustic communication; Gradient climbing; Extremum seeking

<https://doi.org/10.1631/FITEE.1700732>

CLC number: TP273

1 Introduction

Seabed platforms have been widely applied to ocean observation projects, such as seafloor observatory networks and hydrological investigations, which usually mount device measuring temperature, salinity, current, and so forth. Most seabed platforms are usually self-contained; therefore, the measurement data cannot be transmitted to the shore station in

real time. The data can be downloaded only when the seabed platforms are retrieved using large ships after a long period of deployment, such as several months or half a year. So, it is clear that there are some deficiencies in the current mode of data collection, such as low efficiency, bad timeliness, and high cost.

In recent years, a new kind of seabed platform mounted acoustic modem has appeared. The measurement data can be transmitted to ships or buoys through underwater acoustic communication (UAC) in real time, and the data can be received by a shore station through wireless or satellite communication devices. In the Ocean Tracking Network Project of Canada, Dalhousie University has worked with the Satlantic Company to design and manufacture a seabed platform with an acoustic modem, and the

[‡] Corresponding author

* Project supported by the National Key R&D Program of China (No. 2017YFC1405203), the National Natural Science Foundation of China (No. 61401111), and the Public Science and Technology Research Funds Projects of Ocean, China (No. 201505005-2)

§ ORCID: Jiu-cai JIN, <http://orcid.org/0000-0002-4425-5297>

© Zhejiang University and Springer-Verlag GmbH Germany, part of Springer Nature 2019

measurement data can be delivered to a mother ship. Using a buoy relay for data collection via UAC, a seabed platform for tsunami warning and ocean observation was deployed in Coral Sea (Lawson et al., 2012). More and more seabed platforms or mooring systems mount acoustic modems, and the data can be collected using ships, buoys, or even unmanned vehicles, such as autonomous underwater vehicle (AUV), remote operated vehicle (ROV), and unmanned surface vehicle (USV) (Murphy et al., 2014; Han et al., 2017; Park et al., 2017).

In the unmanned vehicle family, USV is a new type of multi-functional surface platform, which has become the focus following the well-known unmanned aerial vehicle (UAV) and AUV (Nad et al., 2015). In the 21st century, more than 40 research teams or departments of ocean technology around the world have fabricated manifold USVs, which have been applied to many oceanic fields, such as bathymetry (Brown et al., 2010), underwater acoustic communication and localization (Bingham et al., 2012), environmental survey (Naeem et al., 2008), marine rescue (Matos et al., 2013), and goal tracking (Sinisterra et al., 2017). Specifically, USV is a kind of surface vehicle which can be a relay or a data collection platform for AUVs, underwater notes, and submarines via UAC technology. In recent years, some USVs have been applied to UAC. The ZARCO USV was developed by the Porto University and designed as a communication relay between air and sea (Santos et al., 2008). Another USV called "Swordfish" was developed by the Porto University and used as a mobile gateway for AUV underwater communication (Martins et al., 2011). The SCOUT USVs fabricated by the Massachusetts Institute of Technology (MIT) were tested for UAC among multi-USV formations. They were designed to be communication relays for AUVs (Curcio et al., 2005). Wave glider without propeller has the potential to be an effective unmanned platform for acoustic communication, and has been tested by the Woods Hole Oceanographic Institution and the University of Hawaii at Manoa (Bingham et al., 2012). An underwater real-time communication system, where the USV relays unmanned underwater vehicle (UUV)'s status and sonar images to a distant base in real time, was developed and tested in Japan (Suzuki et al., 2015). USVs' dynamic pursuit using underwater acoustics was

designed and tested (Reed et al., 2016). In the above work, contributions contain mainly tests and applications for USV acoustic communication technology and USV cooperation with other vehicles (such as AUVs) through UAC. As far as we know, the adaptive data collection scheme for a seabed platform using a USV is first proposed in this study, aiming to solve data transmission for seabed platforms in real time and to raise its efficiency.

Seawater is a kind of non-ideal loss medium for UAC, and the underwater acoustic channel is an extremely complicated channel, which is simultaneously confined by time-space-frequency parameters. The complication of the underwater acoustic channel will lead to instability of acoustic communication in real environments. So, some difficulties still exist. For example, the best communication point does not always coincide with the nearest point from the seabed platform. Such a point may be time-variant. It is obvious that seeking the best communication point around the seabed platform is difficult for a single USV. Although the UAC's link strength field around the seabed platform to a USV is unknown, it can be measured by the USV in real time. So, the problem is how to seek the extremum for unmanned vehicles in an unknown environment. To solve this problem, multiple vehicles were usually used to estimate the field by measurement from neighbors, thus guiding vehicles to arrive at the extremum point of the field (Hollinger et al., 2012). Choi et al. (2009) presented a novel class of self-organizing autonomous sensing agents that form a swarm and learn the static field of interest through noisy measurement from neighbors for gradient climbing. Autonomous mobile sensor networks were employed to measure large-scale environmental fields, and an optimal strategy for mission design addressing both cooperative motion control and cooperative sensing was developed for multiple sensor platforms to explore a noisy scalar field in the plane (Zhang and Leonard, 2010). Gradient climbing was widely applied to cooperative control of multiple vehicles (Bachmayer and Leonard, 2002; Ögren et al., 2004; Biyik and Arcak, 2008; Khong et al., 2015). An adaptive-step-control strategy for autonomous chemical plume tracking (CPT) in both two-dimensional (2D) and three-dimensional (3D) spaces by multiple vehicles was proposed and simulated (Gao et al., 2016). In the above work,

multiple vehicles or mobile sensors were cooperatively controlled to estimate the measurement field, and this mode can cooperatively measure the field and simultaneously seek the extremum and frontal surface (Fig. 1a). However, if only a single vehicle is used to seek the extremum for a field, there is a question of how to design a control scheme. A single vehicle usually cannot rapidly estimate the field because of the limited extent of measurement; therefore, it is difficult for a single vehicle to seek the extremum point. We intend to design a motion style for vehicles to solve this problem. In this study, an oscillation motion (OM) for a single USV is designed to acquire data around the seabed platform and the USV, and to iterate the UAC's link strength field. We desire a USV that can be guided to the best communication point at the same time, which is shown in Fig. 1b.

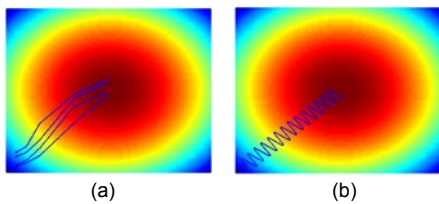


Fig. 1 Extremum seeking: (a) multi-vehicle cooperation; (b) a single vehicle oscillation motion

2 Field estimation for UAC's link strength

2.1 Oscillation motion for USV

A USV is a kind of surface vehicle that can be treated as a self-propelled particle in the plane; therefore, motion equations can be expressed as

$$\dot{\mathbf{r}} = \mathbf{v}, \quad (1)$$

$$\dot{\mathbf{v}} = \mathbf{u}, \quad (2)$$

where the vector $\mathbf{r}=x+iy$ represents the position of the USV, \mathbf{v} the velocity, and \mathbf{u} the steering control variable for the velocity (\mathbf{r} , \mathbf{v} , and $\mathbf{u} \in \mathbb{C}$). Discrete equations for the USV are given as follows:

$$\mathbf{r}(t + \delta) = \mathbf{r}(t) + \mathbf{v}(t)\delta, \quad (3)$$

$$\mathbf{v}(t + \delta) = \mathbf{v}(t) + \mathbf{u}(t)\delta, \quad (4)$$

where δ represents the time interval.

Eqs. (1) and (2) denote that the USV is controlled by the control variable \mathbf{u} in the plane, and that

the model is adaptable for most USVs which are usually steered by speed difference of thrusters or rudder angles. In USV data collection, although the UAC link strength field around the seabed platform is unknown in advance, it can be measured by the USV during data collection in real time. To estimate the gradient of the field strength, the USV should measure the UAC's link strength around the USV as much as possible. So, an OM of the USV is designed to enlarge the measurement extent. The steering control variables are designed as follows:

$$\mathbf{v}(t) = \begin{bmatrix} \cos \varphi & -\sin \varphi \\ \sin \varphi & \cos \varphi \end{bmatrix} \begin{bmatrix} u_0 \\ u_0 A_0 \cos(t/T) \end{bmatrix}, \quad (5)$$

$$\mathbf{u}_1(t) = \begin{bmatrix} \cos \varphi & -\sin \varphi \\ \sin \varphi & \cos \varphi \end{bmatrix} \begin{bmatrix} 0 \\ -u_0 A_0 \frac{\sin(t/T)}{T} \end{bmatrix}, \quad (6)$$

where φ represents the OM's direction of the USV, and A_0 , T , and u_0 represent the oscillation amplitude, period, and velocity, respectively. Simulation results of the OM along with 30° are shown in Fig. 2.

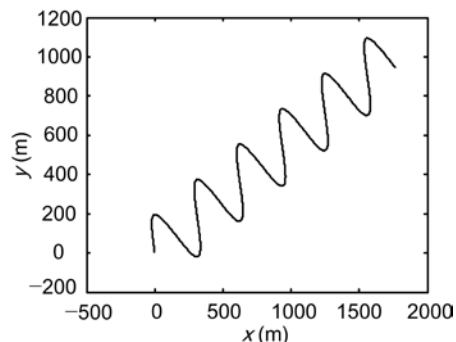


Fig. 2 USV's oscillation motion along with 30° with $\varphi=30^\circ$, $u_0=1$, $A_0=3$, and $T=180/\pi$

2.2 Link strength model for UAC

The decline of acoustic signal strength between vehicles and seabed platforms can be characterized mainly by three factors: attenuation that increases with signal frequency, time-varying multi-path propagation, and Doppler effect for low speed of sound (Stojanovic and Preisig, 2009). However, there are no standardized models for acoustic channel fading, and some statistical models are usually built based on experimental data. The availability of the large experimental data sets is important for

advancement because of the realism compared with models (Stojanovic and Freitag, 2013). In this study, acoustic signal loss is estimated by an empirical formula (Stojanovic, 2006), expressed as

$$A(l, f) = \left(\frac{l}{l_r} \right)^{k_1} a(f)^{l-l_r}, \quad (7)$$

where $a(f)$ is an absorption coefficient, f the signal frequency, l the transmission distance taken in reference to a distance constant l_r , and k_1 the path loss exponent which models the spreading loss. It can be seen that the acoustic signal loss is decided mainly by f and l . The acoustic signal loss after taking a log operation of A , i.e., $\log A$, is approximately proportional to the transmission distance l , and the relationship was manifested by the experimental data in Jin et al. (2016). According to the relationship between the acoustic signal loss and transmission distance, a model for link strength in the form of probability was defined based on the experimental data in Jin et al. (2016)

$$P(\mathbf{r}) = \frac{Q - k_2 \|\mathbf{r} - \mathbf{r}_0\|}{Q} + e, \quad (8)$$

where $P(\mathbf{r})$ is the link strength of UAC, Q the largest signal strength between a USV and a seafloor platform, \mathbf{r}_0 the position of the seabed platform, and e the noise. The defined link strength represents the UAC's quality between the seabed platform and the USV. This is used to be an evaluation index of the best communication location for the USV around the seabed platform. In July 2015, the underwater acoustic communication experiments were implemented using an unmanned surface bathymetry vehicle (USBV) (Fig. 3) at Jihongtan Reservoir, Qingdao, China. The USBV was equipped with an EvoLogics 18/34 acoustic modem, where the acoustic frequency was between 18 and 34 kHz (Jin et al., 2016). Data acquired by the USBV was used to model the link strength. The relationship between the signal strength and the transmission distance is shown in Fig. 4a, and the link strength is shown in Fig. 4b, where the largest signal strength is 84 dB and k_2 is 28 dB/km.

2.3 Estimation for link strength field

The communication link strength between a seabed platform and a USV can be described by a



Fig. 3 An unmanned surface bathymetry vehicle (USBV)

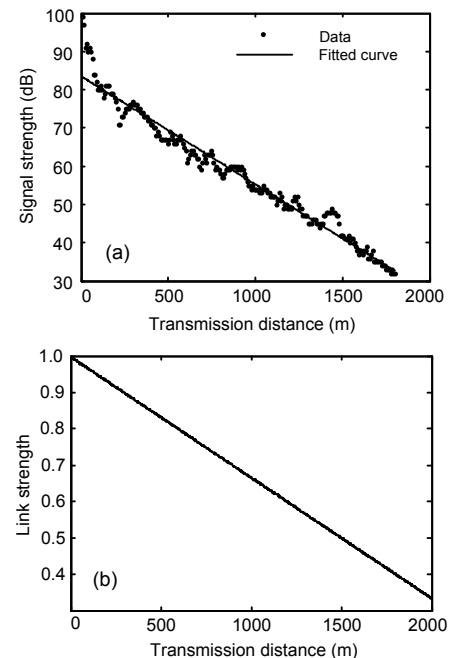


Fig. 4 UAC signal strength and link strength for USV with communication distance: (a) signal strength; (b) link strength

scalar field. The scalar field is unknown and variable because of the complex nature of the acoustic channel and the ocean environments discussed in Section 2.2. To seek the extremum of the field, the scalar field must be updated in real time by new measurement data from the USV. An iteration algorithm is introduced to estimate the scalar field in this subsection.

In the plane $\mathcal{R} \in \mathbb{R}^2$, $z(\mathbf{r}(t))$ is the measured value at position $\mathbf{r}(t)$, and is composed of the scalar value $c(\mathbf{r}(t))$ and the measurement noise $e(\mathbf{r}(t))$, expressed as

$$z(\mathbf{r}(t)) = c(\mathbf{r}(t)) + e(\mathbf{r}(t)), \quad (9)$$

where $c: \mathcal{R} \times R_+ \rightarrow [0, c_{\max}]$ denotes the scalar field in

the plane \mathcal{R} . Note that both the scalar value $c(\mathbf{r}(t))$ and the measurement value $z(\mathbf{r}(t))$ represent the link strength value $P(\mathbf{r}(t))$ for convenience.

Suppose that the scalar field $c(\mathbf{r}(t))$ can be defined using multi-variable linear regression as

$$c(\mathbf{r}(t)) = \sum_{i=1}^m h_i(\mathbf{r}(t))x_i = \mathbf{h}^T(\mathbf{r}(t))\mathbf{x}, \quad (10)$$

where $\mathbf{x}:=(x_1, x_2, \dots, x_m)^T \in \mathbb{R}^m$ is the regression coefficient, $\mathbf{h}(\mathbf{r}(t)):=(h_1, h_2, \dots, h_m)^T$ the base function, and

$h_j(\mathbf{r}(t)):=\frac{1}{a}\exp\left(-\frac{\|\mathbf{r}-\mathbf{b}_j\|^2}{\sigma^2}\right)$ with a a normalization constant and \mathbf{b}_j uniformly locating in the area of $\mathcal{R}, j \in \{1, 2, \dots, m\}$.

The measurement value at $\mathbf{r}(t)$ can be described as $z(\mathbf{r}(t))=\mathbf{h}^T(\mathbf{r}(t))\mathbf{x}+e(\mathbf{r}(t))$. Though the link strength in Fig. 4 is linear to the communication distance, the measurement error $e(\mathbf{r}(t))$ of link strength is not linear to the transmission distance, and the measurement error depends mainly on the ocean environments; therefore, the weight estimation method is used in the regression. The regression coefficient \mathbf{x} can be calculated by the regression criterion for the minimum of the weight residual error based on the data set $\{z(r_k), \mathbf{h}(r_k)\}_{k=1}^N$. The regression criterion J is expressed as

$$J = \sum_{k=1}^N w_k (z(r_k) - \mathbf{h}^T(r_k)\mathbf{x})^2, \quad (11)$$

where w_k is a weight factor and N the total number of measurements. Eq. (11) can also be expressed as

$$J = (z - \mathbf{H}\bar{x})^T \mathbf{W} (z - \mathbf{H}\bar{x}), \quad (12)$$

where \mathbf{W} is an $m \times m$ symmetric matrix called the “weight matrix.”

The condition for the minimum of J is

$$\frac{\partial^2 J}{\partial^2 \mathbf{x}} = 2(\mathbf{H}^T \mathbf{W} \mathbf{H}) > 0, \quad (13)$$

so, $\mathbf{H}^T \mathbf{W} \mathbf{H}$ must be definitely positive.

For the data set $\{z(r_k(t)), \mathbf{h}(r_k(t))\}_{k=1}^N$, $z(k):=z(r_k)$, and $\mathbf{h}(k):=\mathbf{h}(r_k)$, when $\partial J / \partial \mathbf{x} = 0$, the optimal regression coefficients can be acquired as follows:

$$\hat{\mathbf{X}} = (\mathbf{H}^T \mathbf{W} \mathbf{H})^{-1} \mathbf{H}^T \mathbf{W} z. \quad (14)$$

When $\mathbf{W} = \mathbf{R}^{-1}$ and $\mathbf{R} = \mathbf{E}(\mathbf{e} \mathbf{e}^T)$, the variance of the evaluation error of \mathbf{x} is a minimum, and $\mathbf{W} = \mathbf{R}^{-1}$ is called an “optimal weight matrix.” In this situation, the evaluation is a Gauss-Markov evaluation, and Eq. (14) can be expressed as

$$\hat{\mathbf{X}}(N) = \mathbf{P}(N) \mathbf{H}^T(N) \mathbf{W}(N) \mathbf{Z}(N), \quad (15)$$

where $\mathbf{P}(s, n) = (\mathbf{H}^T(s, n) \mathbf{W}(s, n) \mathbf{H}(s, n))^{-1} \in \mathbb{R}^{m \times m}$, $\mathbf{H}(s, n) = (h(s), h(s+1), \dots, h(n))^T \in \mathbb{R}^{(n-s+1) \times m}$, $\mathbf{W}(s, n) = \mathbf{R}^{-1}(s, n) = \mathbf{E}(\mathbf{e}(s, n) \mathbf{e}(s, n)^T)^{-1} \in \mathbb{R}^{(n-s+1) \times (n-s+1)}$, and $\mathbf{Z}(s, n) = (z(s), z(s+1), \dots, z(n))^T \in \mathbb{R}^{n-s+1}$.

Note that $\mathbf{P}(1, N)$ is simplified to $\mathbf{P}(N)$, $\mathbf{H}(1, N)$ is simplified to $\mathbf{H}(N)$, and $\mathbf{Z}(1, N)$ is simplified to $\mathbf{Z}(N)$ in Eq. (15).

According to Eq. (15), the scalar field $c(\mathbf{r}(t))$ can be regressed using the whole measurement data set from the USV. However, the scalar field $c(\mathbf{r}(t))$ should be updated to guide the USV to seek the extremum in real time. Therefore, the estimated field should be iterated using new measurement data based on history data. Let $\mathbf{Z}(N)$ be the history data of the USV measurement before t , and $\mathbf{Z}(N+1, N+T)$ be the new data in the next period of the OM of the USV. For convenience, it is defined as $\mathbf{Z}(j) := \mathbf{Z}(N)$, $\mathbf{Z}(j, j+1) := \mathbf{Z}(N+1, N+T)$, and $\mathbf{H}(j, j+1) := \mathbf{H}(N+1, N+T)$. Iteration equations for the OM of the USV in the period T are given as follows (Zhou and Lu, 2009):

$$\hat{\mathbf{X}}(j+1) = \hat{\mathbf{X}}(j) + \mathbf{K}(j+1)[\mathbf{Z}(j, j+1) - \mathbf{H}(j, j+1)\hat{\mathbf{X}}(j)], \quad (16)$$

where $\mathbf{K}(j+1) = \mathbf{P}(j) \mathbf{H}^T(j, j+1) (\mathbf{W}^{-1}(j, j+1) + \mathbf{H}(j, j+1) \cdot \mathbf{P}(j) \mathbf{H}^T(j, j+1))^{-1}$ and $\mathbf{P}(j+1) = (1 - \mathbf{K}(j+1) \mathbf{H}(j, j+1)) \mathbf{P}(j)$. It can be seen from Eq. (16) that the newly estimated variable $\hat{\mathbf{X}}(j+1)$ is the sum of the previously estimated variable $\hat{\mathbf{X}}(j)$ and a linear revising term between new measurement data $\mathbf{Z}(j+1)$ and $\mathbf{H}(j, j+1)\hat{\mathbf{X}}(j)$.

To obtain an initial field, one selection is based on history data using Eq. (15), and the other selection is to choose some initial values, such as $\mathbf{H}(t)=0$ and $\mathbf{P}(0)=C_1^2 \mathbf{I}$, where C_1 is a constant. The advantage of the second selection is that the iteration can be executed from the first time and does not need to acquire an inverse matrix for $\mathbf{H}^T(t)W(t)\mathbf{H}(t)$.

The new scalar field can be continuously updated by iteration (16) using new measurement data from the USV, expressed as follows:

$$\hat{c}(n, \mathbf{r}) := \mathbf{H}^T(\mathbf{r})\hat{\mathbf{X}}(n). \quad (17)$$

The gradient of the field can be expressed as

$$\nabla \hat{c}(n, \mathbf{r}) = \mathbf{H}'^T(\mathbf{r})\hat{\mathbf{X}}(n) \in \mathbb{R}^{2 \times 1}. \quad (18)$$

3 Controller design and convergence analysis

In the previous section, the instantaneous field for link strength between a seabed platform and a USV is built using the measurement data from the USV. To conveniently illustrate the problem, let $\mathbf{x}=[\mathbf{r}, \mathbf{v}]^T$; so, the state function of the USV can be described as follows:

$$\mathbf{x} = [\mathbf{r}^T, \mathbf{v}^T]^T, \quad (19)$$

$$\dot{\mathbf{x}} = [\mathbf{v}^T, \mathbf{u}^T]^T. \quad (20)$$

Here, two assumptions are given as follows:

1. Parameters u_0 , A_0 , and T are bounded in Eqs. (5) and (6), and all the parameters are larger than zero, assuring an OM for the USV.

2. The initial position of the USV is not on the area boundary of \mathbf{r}_c . If the condition does not hold, the area boundary should be enlarged based on the initial position of the USV.

Select a candidate Lyapunov function as

$$V(x) = \mathbf{U} + \mathbf{c} + \frac{1}{2}\mathbf{v}^T\mathbf{v}, \quad (21)$$

where $\mathbf{U} = \frac{1}{2}k_3(\mathbf{r}(t) - \mathbf{r}_0)^2 + \frac{k_4}{(\mathbf{r} - \mathbf{r}_c)^2}$ is a potential function, the first term of which denotes an attraction potential function and the second term of which

denotes a rejection potential function, \mathbf{r}_0 is the rough location of the seabed platform, and \mathbf{r}_c is the area boundary around the seabed floor. It is clear that $V(x) > 0$.

Then the derivative of $V(x)$ is

$$\dot{V} = (\partial V / \partial \mathbf{x})^T \dot{\mathbf{x}} = [\nabla \mathbf{U} + \nabla \mathbf{c}, \mathbf{v}^T][\mathbf{v}^T, \mathbf{u}^T]^T. \quad (22)$$

Considering the OM of the USV and gradient of the field, the gradient climbing controller is designed as follows:

$$\mathbf{u} = 2 \sin(2t/T) \cdot \mathbf{u}_1 - \nabla \hat{c}(n, \mathbf{r}) - \nabla \mathbf{U}, \quad (23)$$

where \mathbf{u}_1 is the OM control term in Eq. (6). So, the derivative of the Lyapunov function is expressed as follows:

$$\begin{aligned} \dot{V} &= [\nabla \mathbf{U} + \nabla \mathbf{c}, \mathbf{v}^T] \\ &\cdot \left[\mathbf{v}^T, (2 \sin(2t/T) \cdot \mathbf{u}_1 - \nabla \hat{c}(n, \mathbf{r}) - \nabla \mathbf{U})^T \right]^T \\ &= 2 \sin(2t/T) \cdot \mathbf{v}^T \cdot \mathbf{u}_1 \\ &= 2 \sin(2t/T) \cdot \left(\begin{bmatrix} \cos \varphi & -\sin \varphi \\ \sin \varphi & \cos \varphi \end{bmatrix} \begin{bmatrix} u_0 \\ u_0 A_0 \cos(t/T) \end{bmatrix} \right)^T \\ &\cdot \begin{bmatrix} \frac{1}{T} u_0 A_0 \sin \varphi \sin(t/T) \\ -\frac{1}{T} u_0 A_0 \cos \varphi \sin(t/T) \end{bmatrix} \\ &= -2 \sin(2t/T) \frac{u_0^2 A_0^2 \sin(t/T) \cos(t/T)}{T} \\ &= -\frac{u_0^2 A_0^2 \sin^2(2t/T)}{T} < 0. \end{aligned} \quad (24)$$

From the Lyapunov function $V(x)$ in Eq. (21), we can know that $V(x)$ is radially unbounded; that is, $V(x) \rightarrow \infty$ when $\|\mathbf{x}\| \rightarrow \infty$. Under the condition of Eqs. (21) and (24), the gradient climbing controller (19) can assure the stability of extremum seeking for the system.

4 Simulation

To simulate the seeking of the best UAC point of the USV, a 2D field for UAC link strength is built based on Eq. (8) with noise e and a random value

below 10% of the largest value of the link strength, as shown in Fig. 5.

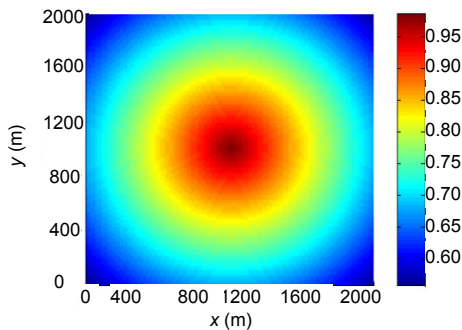
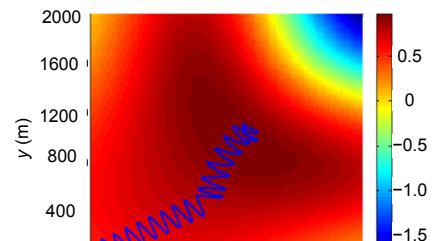


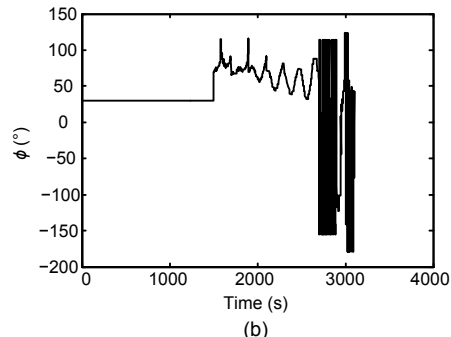
Fig. 5 UAC link strength field between the seabed platform and the USV

In the simulation, the USV is first controlled by an OM controller along with a fixed direction, and its measurement data is regressed as an initial field. Then the simulation goes into the gradient climbing control mode, the proposed controller is used to guide the USV, and the new data of the USV's OM in the next period is added to the iteration of the field. In the first case study, the USV is controlled by the OM controller along with 30° in 1500 s, and the gradient control is executed between 1500 s and 3100 s (Fig. 6). In the simulation, $A_0=6$, $T=90/\pi$, $u_0=0.5$, and $k_3=1$. In Fig. 6a, the blue path of USV converges to the maximum value area of the strength field from the initial point denoted by a circle in the left bottom corner. The oscillation direction for the USV is shown in Fig. 6b, which reflects the USV's seeking process. Before 1500 s, the USV's oscillation direction is fixed at 30° , and measurement data in this period is used for the initial field. The USV's autonomous seeking process is between 1500 s and 3100 s, and the USV finds the extremum area at 2700 s. Between 1500 s and 2700 s, the USV's course changes between 30° and 120° , and the USV continuously tends to the extremum area. After 2700 s, the USV's course fluctuates largely (Fig. 6). This denotes that the USV has hovered around the extremum area. In Fig. 6a, it can be seen that the estimated field is similar to the real field (Fig. 5) around the path of the USV; however, there are some differences for these two fields in the right corner, because the area is far from the measurement range for the USV. Although there are differences between the estimated and the real fields, the

USV can get to the area of the field's maximum point based on the estimated field, demonstrating the validity of the proposed algorithm.



(a)



(b)

Fig. 6 Seeking the best UAC point of the USV with 10% of noise in the first case study: (a) USV trajectory; (b) USV course

References to color refer to the online version of this figure

Figs. 6–8 show the results of seeking the best UAC point of the USV with 10%, 30%, and 50% of noise, respectively. In these cases, the best UAC point can all be found. However, differences between the estimated and real fields of the link strength are enlarged along with the enlargement of noise.

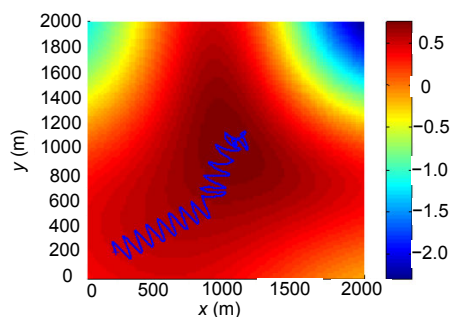


Fig. 7 Seeking for the best UAC point of the USV with 30% of noise

References to color refer to the online version of this figure

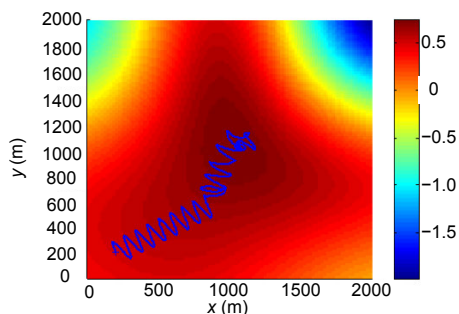


Fig. 8 Seeking the best UAC point of the USV with 50% of noise

References to color refer to the online version of this figure

To validate the proposed algorithm, the second case study is carried out, where the initial oscillation direction of the USV is fixed along with the x axis. In Fig. 9, the USV's oscillation direction is fixed at 0° before 2000 s, and the best UAC point of the USV is found at 3700 s. After 3700 s, the best UAC point of the USV is found, and the “hovering motion” comes out the same as in Fig. 6a.

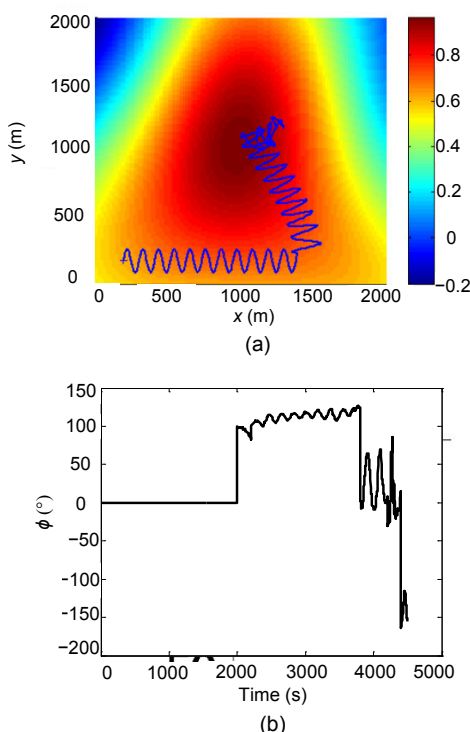


Fig. 9 Seeking the best UAC point of the USV with 10% of noise in the second case study: (a) USV trajectory; (b) USV course

References to color refer to the online version of this figure

In Figs. 6–9, although the initial oscillation motion for the USV does not point to the maximum point, the best UAC point of the USV is found using the proposed controller. In addition, the simulation results are not affected by the disparity between the estimated and real fields, especially in the corners without measurement data from the USV.

5 Conclusions

In underwater data collection applications, more and more unmanned vehicles have been taken as relay nodes. In this study, an algorithm for seeking the extremum area of the UAC link strength field between the USV and the seabed platform has been presented. A controller based on gradient climbing and oscillation motion has been designed and applied to find the best communication point for a single USV without prior knowledge. In the simulation, the proposed algorithm can force a USV to track the best communication area in an unknown UAC link strength field, which is estimated at the same time. The simulation results showed the reliability and efficiency of the algorithm. Future work will investigate how seabed platform network data can be efficiently collected based on a single USV.

Compliance with ethics guidelines

Jiu-cai JIN, Jie ZHANG, and Zhi-chao LV declare that they have no conflict of interest.

References

- Bachmayer R, Leonard NE, 2002. Vehicle networks for gradient descent in a sampled environment. Proc 41st IEEE Conf on Decision and Control, p.112-117. <https://doi.org/10.1109/cdc.2002.1184477>
- Bingham B, Kraus N, Howe B, et al., 2012. Passive and active acoustics using an autonomous wave glider. *J Field Robot*, 29(6):911-923. <https://doi.org/10.1002/rob.21424>
- Biyik E, Arcak M, 2008. Gradient climbing information via extremum seeking and passivity-based coordination rules. *Asian J Contr*, 10(2):201-211. <https://doi.org/10.1002/asjc.19>
- Brown H, Jenkins L, Meadows G, et al., 2010. *BathyBoat*: an autonomous surface vessel for stand-alone survey and underwater vehicle network supervision. *Mar Technol Soc J*, 44(4):20-29. <https://doi.org/10.4031/mtsj.44.4.5>
- Choi J, Oh S, Horowitz R, 2009. Distributed learning and cooperative control for multi-agent systems. *Automatica*, 45(12):2802-2814. <https://doi.org/10.1016/j.automatica.2009.09.025>

- Curcio J, Leonard J, Vaganay J, et al., 2005. Experiments in moving baseline navigation using autonomous surface craft. IEEE Conf on OCEANS, p.730-735.
<https://doi.org/10.1109/OCEANS.2005.1639839>
- Gao B, Li HB, Li W, et al., 2016. 3D Moth-inspired chemical plume tracking and adaptive step control strategy. *Adapt Behav*, 24(1):52-65.
<https://doi.org/10.1177/1059712315623998>
- Han GJ, Li SS, Zhu CS, et al., 2017. Probabilistic neighborhood-based data collection algorithms for 3D underwater acoustic sensor networks. *Sensors*, 17(2):316.
<https://doi.org/10.3390/s17020316>
- Hollinger GA, Choudhary S, Qarabaqi P, et al., 2012. Underwater data collection using robotic sensor networks. *IEEE J Sel Areas Commun*, 30(5):899-911.
<https://doi.org/10.1109/JSAC.2012.120606>
- Jin JC, Zhang J, Lv ZC, et al., 2016. Active and passive underwater acoustic application using an unmanned surface vehicle. IEEE Conf on OCEANS, p.1-6.
<https://doi.org/10.1109/oceansap.2016.7485378>
- Khong SZ, Tan Y, Manzie C, et al., 2015. Extremum seeking of dynamical systems via gradient descent and stochastic approximation methods. *Automatica*, 56:44-52.
<https://doi.org/10.1016/j.automatica.2015.03.018>
- Lawson RA, Graham D, Stalin S, et al., 2012. The next generation Easy-to-Deploy (ETD) tsunami assessment buoy. IEEE Conf on OCEANS, p.1-8.
<https://doi.org/10.23919/OCEANS.2011.6107114>
- Martins R, de Sousa JB, Afonso CC, et al., 2011. REP10 AUV: shallow water operations with heterogeneous autonomous vehicles. IEEE Conf on OCEANS, p.1-6.
<https://doi.org/10.1109/Oceans-Spain.2011.6003568>
- Matos A, Silva E, Cruz N, et al., 2013. Development of an unmanned capsule for large-scale maritime search and rescue. IEEE Conf on OCEANS, p.1-8.
<https://doi.org/10.23919/OCEANS.2013.6741340>
- Murphy C, Walls JM, Schneider T, et al., 2014. CAPTURE: a communications architecture for progressive transmission via underwater relays with eavesdropping. *IEEE J Ocean Eng*, 39(1):120-130.
<https://doi.org/10.1109/JOE.2013.2261331>
- Nad Đ, Mišković N, Mandić F, 2015. Navigation, guidance and control of an overactuated marine surface vehicle. *Ann Rev Contr*, 40:172-181.
<https://doi.org/10.1016/j.arcontrol.2015.08.005>
- Naeem W, Xu T, Sutton R, et al., 2008. The design of a navigation, guidance, and control system for an unmanned surface vehicle for environmental monitoring. *Proc Inst Mech Eng M-J Eng Mar Environ*, 222(2):67-79.
<https://doi.org/10.1243/14750902JEME80>
- Ögren P, Fiorelli E, Leonard NE, 2004. Cooperative control of mobile sensor networks: adaptive gradient climbing in a distributed environment. *IEEE Trans Automat Contr*, 49(8):1292-1302.
<https://doi.org/10.1109/TAC.2004.832203>
- Park JH, Kang MJ, Kim TY, et al., 2017. Development of an unmanned surface vehicle system for the 2014 Maritime RobotX Challenge. *J Field Robot*, 34(4):644-665.
<https://doi.org/10.1002/rob.21659>
- Reed BL, Leighton J, Stojanovic M, et al., 2016. Multi-vehicle dynamic pursuit using underwater acoustics. In: Inaba M, Corke P (Eds.), *Robotics Research*. Springer Tracts in Advanced Robotics. Springer Press, Berlin, Germany, p.79-94. https://doi.org/10.1007/978-3-319-28872-7_5
- Santos N, Matos A, Cruz N, 2008. Navigation of an autonomous underwater vehicle in a mobile network. IEEE Conf on OCEANS, p.1-5.
<https://doi.org/10.1109/OCEANS.2008.5151980>
- Sinisterra AJ, Dhanak MR, von Ellenrieder K, 2017. Stereovision-based target tracking system for USV operations. *Ocean Eng*, 133:197-214.
<https://doi.org/10.1016/j.oceaneng.2017.01.024>
- Stojanovic M, 2006. On the relationship between capacity and distance in an underwater acoustic communication channel. Proc 1st ACM Int Workshop on Underwater Networks, p.41-47.
<https://doi.org/10.1145/1161039.1161049>
- Stojanovic M, Freitag L, 2013. Recent trends in underwater acoustic communications. *Mar Technol Soc J*, 47(5):45-50. <https://doi.org/10.4031/MTSJ.47.5.9>
- Stojanovic M, Preisig J, 2009. Underwater acoustic communication channels propagation models and statistical characterization. *IEEE Commun Mag*, 47(1):84-89.
<https://doi.org/10.1109/MCOM.2009.4752682>
- Suzuki N, Kitajima H, Kaba H, et al., 2015. An experiment of real-time data transmission of sonar images from cruising UUV to distant support vessel via USV: development of underwater real-time communication system (URCS) by parallel cruising. IEEE Conf on OCEANS, p.1-6.
<https://doi.org/10.1109/OCEANS-Genova.2015.7271465>
- Zhang FM, Leonard NE, 2010. Cooperative filters and control for cooperative exploration. *IEEE Trans Automat Contr*, 55(3):650-663.
<https://doi.org/10.1109/TAC.2009.2039240>
- Zhou FQ, Lu XD, 2009. *Theory of Optimal Estimation*. Higher Education Press, Beijing, China, p.16-19 (in Chinese).